35th International Conference on Lightning Protection
XVI International Symposium on Lightning Protection
20th to 24th September 2021 - Sri Lanka
ICLP-SIPDA SRI LANKA 2021

Space-leader characteristics in negative stepped-leaders followed by return strokes with significantly different peak currents

Hamza Khounate, Amitabh Nag, Mathieu N. Plaisir,
Abdullah Y. Imam and Hamid K. Rassoul
Department of Aerospace, Physics and Space Sciences
Florida Institute of Technology
Melbourne, Florida

Christopher J. Biagi
NASA
Kennedy Space Center
Titusville, Florida
USA

***Abstract*— We present sub-microsecond-scale, high-speed video camera observations of three negative stepped leaders in cloud-to-ground flashes with return-stroke peak currents (estimated by the U.S. National Lightning Detection Network) of -17, -104, and -228 kA. The camera frame exposure times for these observations were 1.8, 1.0 and 0.8 µs, respectively. The 0.8 µs exposure time is the shortest reported to date. We observed the temporal and spatial evolution of space leaders from their inception to their attachment to the pre-existing leader channel (PELC). For stepped leaders that led to return strokes having higher peak currents, the space leaders appear to have incepted at farther median two-dimensional distances from their respective PELC-attachment points. These median distances were 6.1, 16.6, and 17.6 m, respectively, for the three strokes. Our observations indicate that space leader characteristics are likely influenced by stepped-leader line-charge-density, which is expected to be higher in strokes with higher return-stroke peak currents.**

KEYWORDS*—*Lightning, Space leader, Cloud-to-ground lightning, Stepped-leader, Peak current, High-speed video camera observations

I. INTRODUCTION

A space stem is a luminous plasma segment that has been observed to form ahead of the leader tip during the negative leader stepping process ([1], [2] and [3]). A space stem may eventually thermalize, undergo a sharp increase in conductivity, and develop into a space leader. Due to the intensification of electric field at its extremities, a space leader can start extending toward the pre-existing leader channel (PELC), eventually connecting with the PELC leading to its extension and the completion of a new leader step. Characterizing the details of the formation and progression of space leaders is, therefore, essential for understanding the leader stepping process as well as the extent to which electrical characteristics of the PELC influence the formation and extension of space leaders. Reference [1] first observed in laboratory spark experiments, space stems which were incepted in the vicinity of the negative leader tip and later evolved into space leaders that merged with the negative primary leader channel, leading to its extension. However, at the time, it was unclear whether the discrepancies in the electrical and geometrical properties between laboratory and lightning leaders would allow for an accurate prediction of the lightning negative leader step formation mechanism from the laboratory experiments. Biagi et al. (2009, 2010) [2, 3] were the first to report separated luminous segments in dart-stepped leaders of triggered lightning flashes using high-speed video cameras; they observed 1-4 m long luminous segments 1-10 m ahead of the leader that they believed were space stems and space leaders. Biagi et al. (2014) [4] observed eight luminous segments 1-6 m in length and 3-8 m ahead of the downward stepped leader preceding the first stroke of an altitude-triggered flash. Hill et al. (2011) and Petersen et al. (2013) [5, 6] each observed in natural cloud-to-ground lightning, luminous segments they called space stems during the stepping process of a downward leader. The luminous segments observed by [5] were on average 3.9 m long and were located around 2 m ahead of the PELC and those reported by [6] were 1-5 m long. Qi et al. (2016) [7] recorded 23 space leaders in a natural lightning stepped-leader occurring 1 to 8 m ahead of the downward leader tip with lengths of 1 to 13 m. Jiang et al. (2017) [8] observed 31 space leaders occurring, on average, 3.6 m ahead of the leader tip. Srivastava et al. (2019) and Qi et al. (2019) [9, 10] reported average space-leader lengths of 2.1 and 3 m, respectively. Table I summarizes the measurement characteristics, lightning type, return-stroke peak current, and observed geometric properties of space stems/leaders reported in these prior studies. Note that all lengths and distances in these studies are two-dimensional (2-D).

In this study, we characterize in detail the formation and evolution of space leaders in three negative cloud-to-ground stepped leaders observed in July-September 2020 using high-speed video cameras operating at 400, 575 and 780 kilo-frames per second. The three stepped-leaders were followed by return strokes with remarkably different peak currents; we examine the

TABLE I. MEASUREMENT CHARACTERISTICS, STROKE-PARAMETERS, AND GEOMETRIC PROPERTIES OF THE OBSERVED SPACE STEMS/LEADERS IN ROCKET-TRIGGERED AND NATURAL LIGHTNING REPORTED IN DIFFERENT STUDIES.

Study	Space stem/leader						
	N	*Length (m)*	*Distance from PELC (m)*[2]	*Frame interstep interval (μs)*	*Observation distance (m)*	*RS peak current (kA)*	*Lightning type*
Biagi et al. (2009) [2]	2	2, 4	4	185, 20	440	-	Rocket-triggered lightning
Biagi et al. (2010) [3]	-	1-4	1-10	4.17	440	-	
Biagi et al. (2014) [4]	8	1-6	3-8	9.26	440	-	
Hill et al. (2011) [5]	16	3.9 (AM)	2.1 (AM)	3.33	1000	-10.6	Natural lightning
Petersen et al. (2013) [6]	-	1-5	-	100	770	-35	
Qi et al. (2016) [7]	23	5 (AM)	4 (AM)	100, 20	350	-	
Jiang et al. (2017) [8]	31	-	3.8 (AM)	5.6	410-1030	-	
Srivastava et al. (2019) [9]	34	2.1 (AM)	-	2.63	910	-19	
Qi et al. (2019) [10]	12	3 (AM)	<2.7 (AM)	1.9	490	-13	
Present study	30	4.3[1] (AM)	6.9 (AM)	2.7	2700	-17	
	22	12.7[1] (AM)	20 (AM)	1.5	7900	-104	
	41	14.4[1] (AM)	24 (AM)	1.2	4900	-228	

(1) The AMs of the maximum observed length of space leaders are provided for all space leaders (that may or may not attach to the PELC).

(2) The AM distances between the observed inception point of space leaders and the PELC-tip are provided for the three negative leaders in this study. In other studies (at least in [2]; [5]; [7] and [10]), it appears that the distance from PELC represents the distance between the space leader's positively charged extremity and the PELC tip, which is likely more dependent (that the inception-point-to-PELC-tip) on the frame rate of the camera. Our AM distance-from-PELC for the 17-kA stroke are, therefore, expectedly somewhat longer than those reported for strokes with similar peak currents in previous studies.

relationship of space-leader characteristics to the respective return-stroke peak current.

II. MEASUREMENT SYSTEM AND DATA

The three stepped leaders analyzed in this study were recorded using high-speed video cameras which are a part of the Melbourne Lightning Observatory (MLO), located on the campus of Florida Institute of Technology in Melbourne, Florida.

The high-speed cameras were installed on a motorized rotating platform on the roof of a five-story building about 18 m above ground level. The pan and tilt features of the platform gave the cameras 340º horizontal and 25º vertical fields-of-view (FOVs).

The first return strokes following all three stepped leaders were geolocated by the U.S. National Lightning Detection Network (NLDN). The first stepped leader, labeled as 070420_17kA in Table II, was part of a single-stroke cloud-to-ground flash that occurred on July 04th, 2020 at 22:26:07 UTC with an NLDN-estimated return-stroke peak current of 17 kA. The stepped leader labeled as 071020_104kA in Table II occurred on July 10th, 2020 at 23:07:22 UTC and was part of a four-stroke flash with the first-stroke peak current being 104 kA. These two stepped leaders had NLDN-reported ground ‑ termination points at distances of 2.7 and 7.9 km from the camera location, respectively. They were measured using a v1210 Phantom high speed video camera, operating at 400 and 575 kilo-frames per second, respectively. The frame exposure times were 1.8 μs and 1 μs, respectively. The third stepped leader, labeled as 09062020_228kA in Table II, occurred on September 6th, 2020 at 17:56:57 UTC and was part of a five-stroke flash with the first return-stroke peak current being 228 kA. The ground-termination point was at a distance of 4.9 km from the camera. It was recorded using a v2512 Phantom high speed video camera operating at 780 kilo-frames per second. The frame exposure time was 0.8 μs, which, to the best of our knowledge, is the shortest reported exposure time used to observe natural lightning leaders to date. Fig. 1 shows the ground-termination points of the three strokes and their distances to the location of the high-speed video cameras. Both cameras were operated with a Nikon 50 mm lens set to an aperture of f/1.8.

TABLE II. NLDN-REPORTED STROKE-PARAMETERS AND CAMERA MEASUREMENT-CHARACTERISTICS FOR THE THREE STROKES.

Stroke ID	**NLDN-estimated**		**Camera characteristics**					
			Frame characteristics			***Pixel resolution (m/pixel)***	***Record length (μs)***	***Altitude range AGL of FOV (m)***
	RS peak current (kA)	***Distance to stroke (km)***	***Interval (μs)***	***Exposure time (μs)***	***Dead time (μs)***			
070420_17kA	-17	2.7	2.5	1.8	0.7	1.5	460	826-922
071020_104kA	-104	7.9	1.7	1.0	0.7	4.4	128	300-440
090620_228kA	-228	4.9	1.2	0.8	0.4	2.8	252	801-978

The video frames were timestamped using a GPS timing system with an accuracy of 10 ns. Note that the NLDN median location errors given by the semimajor axis length of the 50% confidence ellipse (e.g., [11]) were 360 m, for the first recorded stroke (070420_17kA) in our dataset and 200 m for both the second and third strokes (071020_104kA and 09062020_228kA, respectively). Also note, the median absolute peak current estimation error for the NLDN is about 14% ([12]; [13]).

Using the NLDN-estimated stroke locations and camera characteristics, we estimated the size of each pixel and the 2-D horizontal (H) and vertical (V) FOVs. These FOVs (H x V) were 195 m x 96 m, 566 m x 141 m, and 354 m x 177 m for the three records, resulting in spatial resolutions of 1.5, 4.4, and 2.8 m, respectively. All lengths/distances estimated from the video frames in this study are 2-D and may be underestimates with respect to their corresponding 3-D values by about 30% ([14]; [15]) The altitudes above ground level (AGL) for our FOVs shown in Table II were estimated using the tilt angle of the camera platform, the altitude AGL of the camera, and the stroke locations. The three stepped leaders, 070420_17kA, 071020_104kA, and 09062020_228kA, were recorded at altitude ranges of 826-922, 300-440, and 801-978 m, respectively.

In this study, a luminous segment (pixel or group of pixels) is considered as containing a space leader if it is separated from the PELC, and if its brightness (gray level value) is larger than that of the pixels in the region between the luminous segment and the PELC. Note that, we did not distinguish between space stems and space leaders; we refer to all luminous segments that were observed around the PELC and unattached to it as space leaders.

III. ANALYSIS AND RESULTS

We observed that space leaders may or may not attach to the PELC. The space leaders that did attach to the PELC may have attached either to its tip leading to its forward extension or to its lateral surface that may have led to the formation of a new

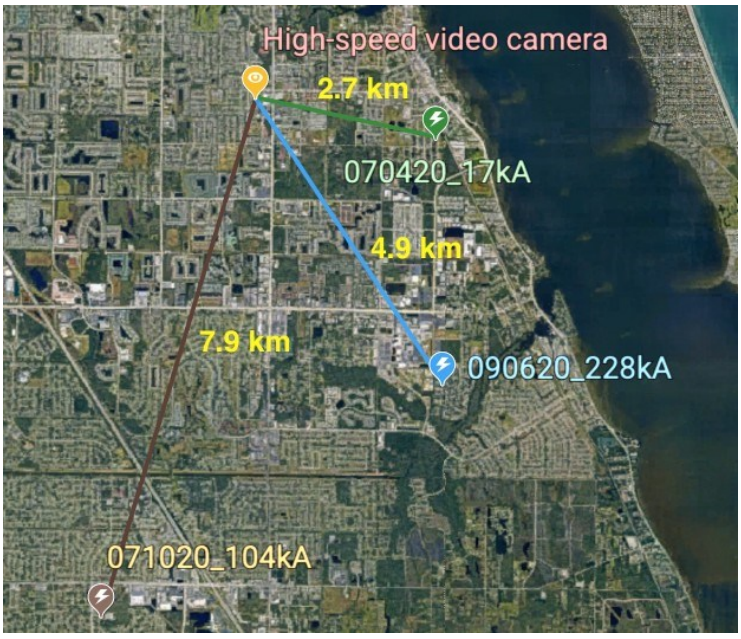

Figure 1. NLDN-reported ground-termination points of the strokes 070420_17kA, 071020_104kA, and 09062020_228kA. The ground-termination points were at distances of 4.9, 2.7 and 7.9 km from the camera location, respectively.

branch (see section III.B below). Fig. 2a-c shows three consecutive frames of the stepped leader 090620_228kA illustrating the three observed stages of space leader evolution: inception, progression, and attachment to the PELC. Each frame captures light for 0.8 μs, followed by a camera dead-time of 426 ns. The frame annotated t ≡ 0 (frame a) shows the inception of a space leader; it is the first frame in which the space leader appears. The next frame (b) starts at t = 1.26 μs and shows the space leader propagating toward the PELC. In the third frame (c) the space leader attaches to the tip of the PELC, leading to the latter's extension by the completion of a new leader step.

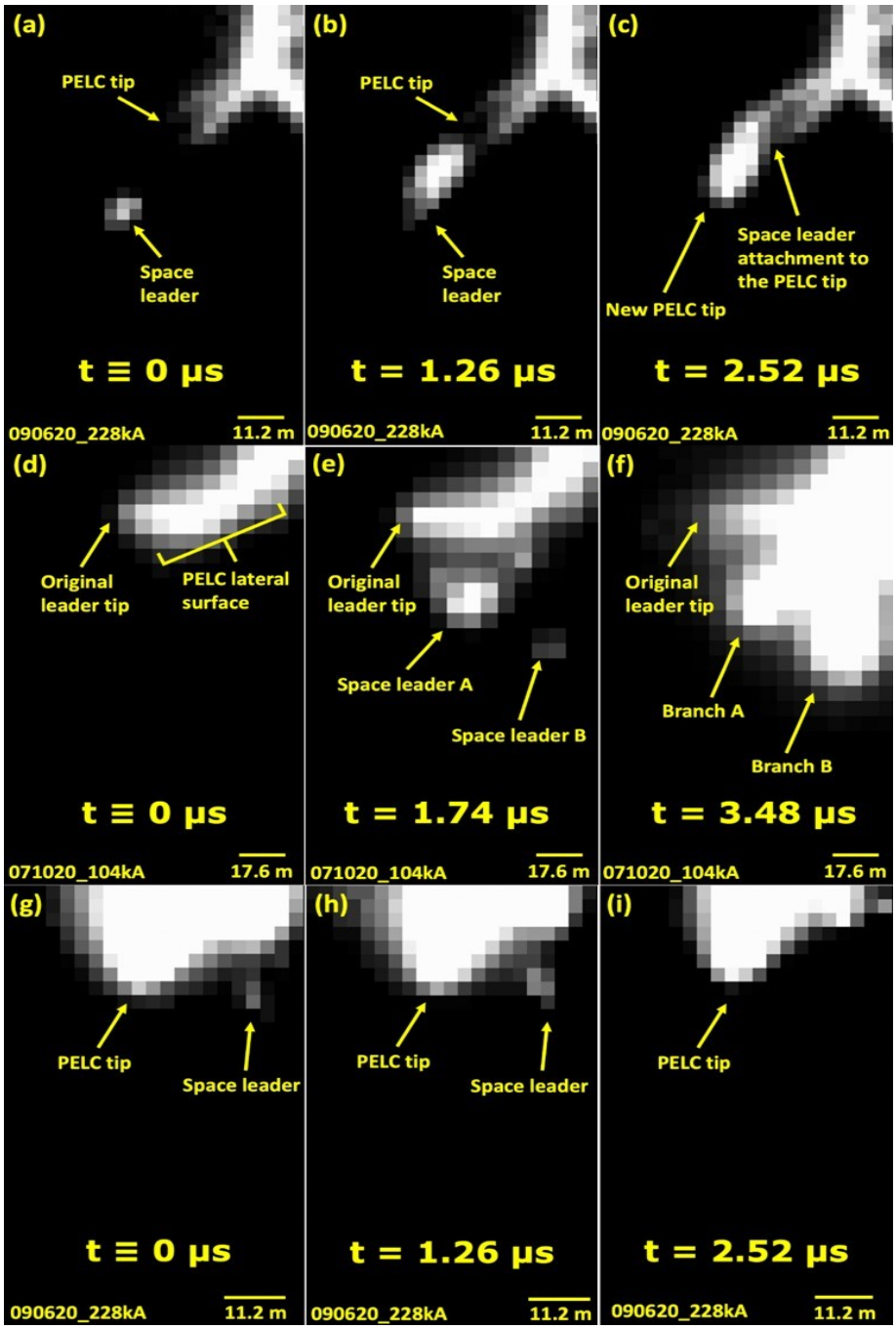

Figure 2. (a-c) Consecutive video-camera frames (exposure time of 0.8 μs) showing inception (a), progression (b), and attachment (c) of a space leader that attached to the PELC tip, in stepped leader 090620_228kA. (d-f) Consecutive frames (exposure time of 1 μs) showing two space leaders (labeled as A and B in (e)) attaching to the PELC-lateral-surface (labeled in (d)) leading to formation of two new branches (f), in stepped leader 071020_104kA. (g-i) Consecutive frames (exposure time of 0.8 μs) showing a space leader incepting (g) in the vicinity of the PELC's lateral surface, its progression (h) toward the PELC, and its disappearance (i) without attaching to the PELC, in stepped leader 090620_228kA.

Fig. 2d-f shows three consecutive frames of the stepped leader 071020_104kA. The frame exposure time is 1 μs, followed by a camera dead-time of 0.7 μs. Frame e, annotated t = 1.74 μs, shows the inception of two space leaders near the lateral surface (labeled in frame d) of the PELC. The next frame (f) starts at t = 3.48 μs and shows the two space leaders attaching to the lateral surface of the PELC and creating two new branches, while the original PELC-tip receded backward.

Fig. 2g-i shows three consecutive frames of the stepped leader 090620_228kA. Frame g, annotated t ≡ 0 μs, shows the inception of a space leader near the lateral surface of the PELC. In frame h, the space leader is observed to have propagated towards the PELC, and 1.26 μs later in frame i, the space leader has disappeared presumably without attaching to either the tip or the lateral surface of the PELC as can be surmised from the observed lack of PELC extension.

A. Space leader inception point location relative to the PELC tip

We estimated the 2-D positions of the inception points of all observed space leaders with respect to the PELC tip. Fig. 3a shows, for the three stepped leaders, the inception points of space leaders that later attached either to the tip (solid symbols) or the lateral surface (hollow symbols) of the PELC. The black line in the figure indicates the reference-line, with its tip located at the origin (0,0) of a two-dimensional plane, along which the PELC associated with each observed space leader was aligned.

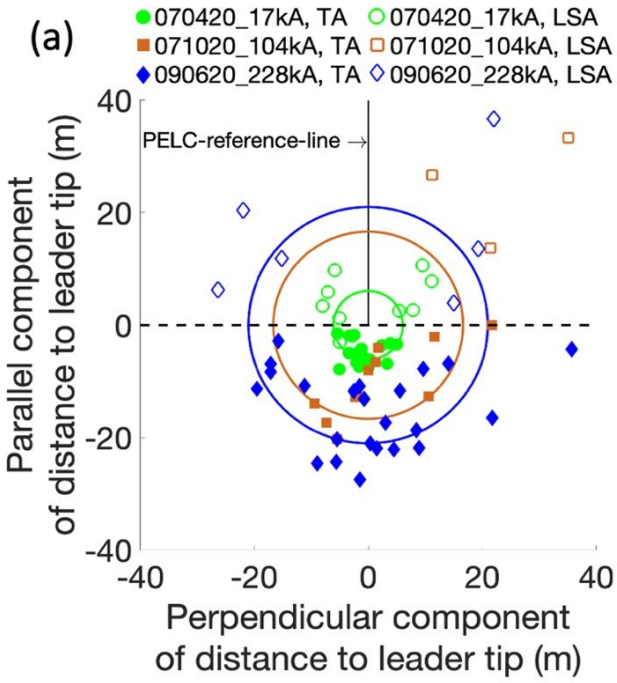

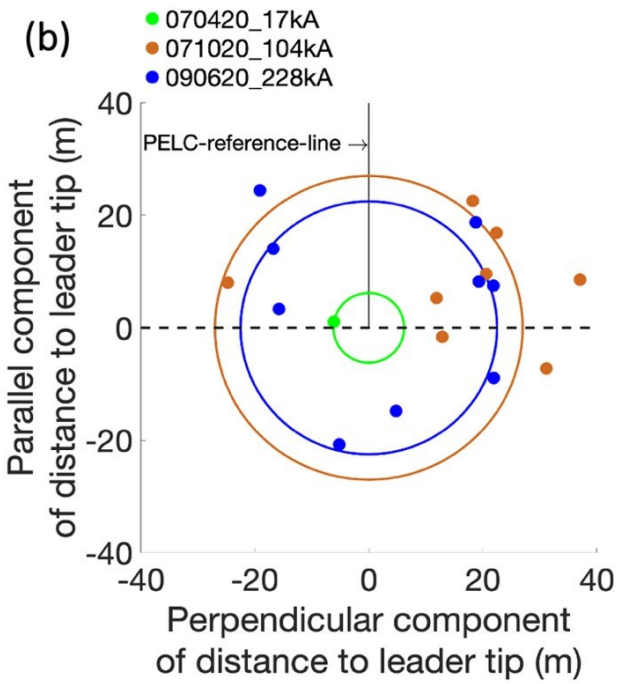

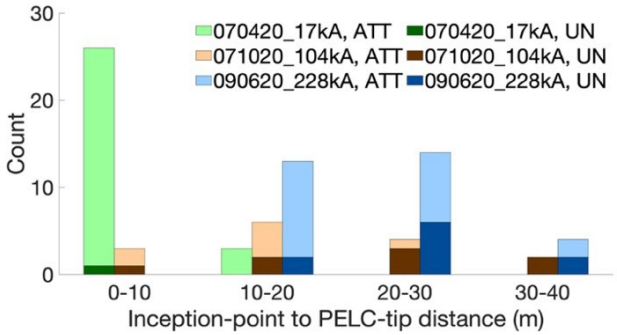

(d)

Stroke ID	070420_17kA		071020_104kA		090620_228kA		All	
Attached [ATT] / Unattached [UN]	ATT	UN	ATT	UN	ATT	UN	ATT	UN
N	29	1	14	8	31	10	74	19
AM (m)	7.0	6.2	18.1	23.3	23.2	26.5	15.9	24.1
Median (m)	6.1	6.2	16.7	27.0	21.0	22.5	13.1	23.1
GM (m)	6.5	6.2	15.3	20.6	21.4	24.3	12.6	21.1
SD (m)	2.7	-	11.1	10.8	10.4	14.2	11.2	12.9
Min (m)	3.0	6.2	4.4	7.5	10.9	15.5	3.0	6.2
Max (m)	14.3	6.2	48.0	38.0	57.8	64.7	57.8	64.7

Figure 3. (a) Inception points of space leaders that later attached either to the tip (solid symbols, labeled TA in the legend) or the lateral surface (hollow symbols, labeled LSA in the legend) of the PELC in the three stepped leaders. The black line indicates the reference-line, with its tip located at the origin (0,0) of a two-dimensional plane, along which the PELC associated with each observed space leader was aligned. The 2-D position of each space leader on this plane was determined by measuring the length of the line joining the inception point of the space leader and the PELC tip as well as the angle between this line and the PELC-reference-line. The radii of the origin-centered circles indicate the median distances of space leader inception points from the PELC-tip for the three space leaders. (b) Same as in (a) but for space leaders that do not attach to the PELC. (c) Bar chart of the space-leader inception-point 2-D distance from PELC-tip for the three stepped leaders. Light and dark shades of the same color indicate space leaders that attached (labeled ATT in the legend) and those that remained unattached (labeled UN in the legend). (d) Sample size (N), Arithmetic mean (AM), median, geometric mean (GM), standard deviation (SD), minimum (Min) and maximum (Max) values for (c) are shown.

The 2-D position of each space leader on this plane was then determined by measuring the length of the line joining the inception point of the space leader and the PELC tip as well as the angle between this line and the PELC-reference-line. We observed 29, 14, and 31 space leaders that attached to the PELC in the stepped leaders 070420_17kA, 071020_104kA, and 09062020_228kA, respectively. The smallest number of space leaders were observed for stepped leader 071020_104kA, which occurred at the farthest distance from the camera. The radii of the origin-centered circles in Fig. 3a indicate the median distances of space leader inception points from the PELC-tip for the three stepped leaders. These median distances were 6.1 m (green circle), 16.7 m (brown circle), and 21 m (blue circle), respectively, for the three stepped leaders. So, space leaders appear to incept at farther median distances from the PELC in stepped leaders that led to return strokes having higher peak currents.

Of the space leaders that attached to the PELC, 20 (69%), 11 (79%), and 23 (74%) attached to its tip in the three stepped leaders, respectively. All such space leaders incepted ahead of the PELC tip (in the lower half-plane of Fig. 3a, below the horizontal dashed line passing through the origin) and contributed to its forward extension. On the other hand, all space leaders that connected to the lateral surface of the PELC, except one (in stepped leader 070420_17kA), incepted behind the PELC tip (i.e., in the upper half-plane of Fig. 3a, above the horizontal dashed line). Such space leaders resulted in the formation of new branches (as shown in Fig. 2d-f) or merged into the lateral surface of the PELC without forming a new branch. The latter scenario occurred when two (or more) "competing" space leaders formed near a PELC, one of which was "preferred" for attachment to the PELC, usually at its tip. Such an attachment was immediately followed by the growth in the diameter of the PELC, leading to the "absorption" of the remaining space leader near its lateral surface. Finally, regardless of the location of a space leader's attachment to the PELC, immediately after attachment, there was a rapid increase in the PELC-brightness due to a luminosity pulse that travelled backward along the PELC and was followed by the brightness gradually (over several microseconds) decreasing to the pre-attachment levels.

As noted earlier, not all space leaders successfully attached to the PELC. One of the optical characteristics observed in our video-camera records that we used to distinguish space leaders that attach to the PELC (including those that merge with the PELC, as discussed above) from those that do not is the absence, in the latter case, of increased brightness of the PELC and the backward moving luminosity pulse that accompanies/follows space-leader-to-PELC attachment. Fig. 3b shows, for the three stepped leaders, the inception points of all the observed space leaders that did not attach to the PELC. We observed 1, 8, and 10 such space leaders for stepped leaders 070420_17kA, 071020_104kA, and 09062020_228kA, respectively. For 070420_17kA, the unattached space leader occurred at a distance of 6.2 m from the PELC tip. For 071020_104kA and 09062020_228kA, the median distances from the PELC-tip were 27 m and 22.5 m, respectively, which are longer than the respective median distances of 16.7 and 21 m for space leaders that attached to the PELC. For all three stepped leaders combined, the median inception-point-to-PELC-tip distances for space leaders that attached to the PELC versus those that did not were 13.1 and 23.1 m, respectively (see Table in Fig. 3d). So, space leaders that did not attach to the PELC were incepted at longer median distances from its tip than those that attached to the PELC. We observed that unattached space leaders may cease propagation toward the PELC and disappear as a result of their relatively large distance to the PELC. In some cases, when multiple simultaneous space leaders were present near a PELC, a closer space leader attached and changed the direction/orientation of the PELC away from the other space leader(s) resulting in them remaining unattached and eventually disappearing. Interestingly, the majority (14 out of 19, i.e., 73%) of the space leaders that remained unattached occurred behind the respective PELC's tip (in the upper half-plane in Fig. 3b). Fig. 3c shows the bar chart of the space-leader inception-point 2-D distance from PELC-tip for the three stepped leaders. For all three stepped leaders combined, the minimum and maximum distances were 3 (in 070420_17kA) and 57.8 m (in 09062020_228kA), respectively, for space leaders that attached to the PELC. For unattached space leaders these were 6.2 (in 070420_17kA) and 64.7 m (in 09062020_228kA), respectively.

B. Space leader inception-point distance from PELC attachment point

Fig. 4a shows the bar chart of the 2-D distance between each space leader's inception point and its attachment point on the PELC. As discussed in section III.A, the PELC-attachment point could either be at the PELC's tip or at its lateral surface. For space leaders that attached to the PELC-tip, the median inception-to-attachment-point distances were 6.1 (N = 20), 16.5 (N = 11), and 20.5 m (N = 23) for stepped leaders 070420_17kA, 071020_104kA, and 09062020_228kA, respectively. For space leaders that attached to the PELC lateral-surface, these median inception-to-attachment-point distances were 7.7 (N = 9), 25.1 (N = 3), and 14.3 m (N = 8) for the three stepped leaders, respectively. For all space leaders that attached to the PELC (regardless of their PELC-attachment-point location, not shown in Fig. 4a), the median inception-to-attachment-point distances were 6.1 (N = 29), 16.6 (N = 14), and 17.6 m (N = 31), respectively, for the three strokes, showing an increase with increasing return-stroke peak current.

C. Space leader 2-D length and leader-step progression speeds

Fig. 4b shows, for the three stepped leaders, the histogram of the maximum observed space leader 2-D lengths. For space leaders that attached to the PELC, these lengths were measured in the video-camera frame immediately preceding the one in which the space leader attached to the PELC. For space leaders that did not attach the PELC, these were the maximum observed space leader lengths. The median values of these lengths were 2.7 and 3.3 times larger for strokes 071020_104kA (median = 11.8 m) and 090620_228kA (median = 14 m), respectively, than that of stroke 070420_17kA (median = 4.3 m). The median leader step-lengths (not shown in Fig. 4b) were 7, 28.5, and 30 m, for the 17 kA, 104 kA, and 228 kA strokes, respectively. The

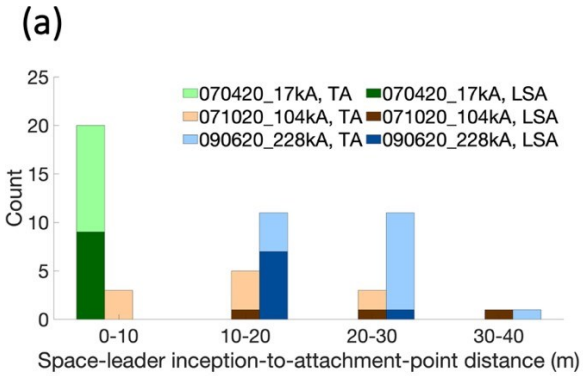

(b)

Stroke ID	070420_17kA		071020_104kA		090620_228kA		All	
Attachment point	TA	LSA	TA	LSA	TA	LSA	TA	LSA
N	20	9	11	3	23	8	54	20
AM (m)	6.0	6.8	14.6	24.3	19.9	14.4	13.7	12.4
Median (m)	6.1	7.7	16.5	25.1	20.5	14.3	12.3	10.1
GM (m)	5.7	6.4	13.0	21.8	19.1	13.9	11.3	10.5
SD (m)	1.6	2.1	6.4	12.6	6.1	4.0	8.0	7.9
Min (m)	3.0	3.5	4.4	11.3	10.9	10.0	3.0	3.5
Max (m)	9.3	9.5	22.7	36.4	36.0	22.7	36.0	36.4

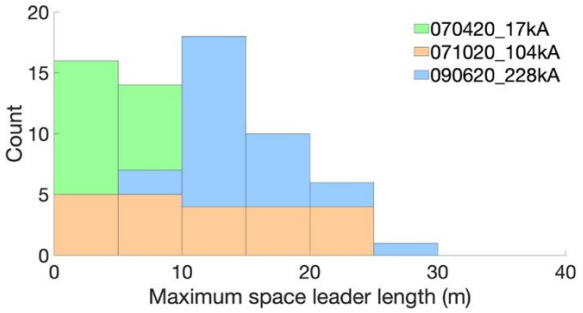

(d)

Stroke ID	070420_17kA	071020_104kA	090620_228kA	All
N	30	22	43	95
AM (m)	4.3	12.7	14.4	10.8
Median (m)	4.3	11.8	14.0	9.5
GM (m)	3.7	10.8	13.3	8.5
SD (m)	2.2	6.8	5.4	6.7
Min (m)	1.5	4.4	4.3	1.5
Max (m)	8.2	24.0	25.8	25.8

Figure 4. (a) Bar chart of 2-D distance between inception and attachment points for space leaders that attached to the PELC-tip (labeled TA in the legend) and to the PELC-lateral surface (labeled LSA in the legend). (b) Histogram of maximum observed space leader 2-D length. See text for more details. Statistics are shown in the tables on the right.

leader-step progression speeds (length divided by formation-time of a newly formed leader step) ranged from 0.1 to 1.1 x 10^6, 1.1 to 4.5 x 10^6, and 0.7 to 3.5 x 10^6 m/s for the three stepped leaders, with the median values being 0.4 x 10^6, 1.7 x 10^6, and 1.4 x 10^6 m/s, respectively.

IV. Discussion and Summary

We reported sub-microsecond-scale optical observations of space leader evolution (inception, progression, and attachment to PELC) in three negative stepped leaders with remarkably different return-stroke peak currents (-17, -104 and -228 kA). To the best of our knowledge, no previous study has reported observations of space leaders in cloud-to-ground lightning with return stroke peak currents comparable to -104 or -228 kA.

Our observation of backward propagating luminosity waves immediately following attachment of space leader to the PELC is consistent with observations of such luminosity waves in rocket triggered lightning (e.g., [16]; [17]), natural lightning (e.g., [5]) and long sparks (e.g., [1]). In Table I we summarize the characteristics of space leaders observed in previous studies and compare them to those obtained in this study. The return stroke peak currents in previous studies ranged from -10.6 to -35 kA. Only one of our stepped leaders had a following return stroke with peak current in this range (-17 kA). For this stepped leader, the AM space leader length and distance from PELC of 4.3 and 6.9 m, respectively, are comparable to those reported in previous studies, however these values are much larger for the other two stepped leaders (with return stroke peak currents of -104 and -228 kA) in this study.

For space leaders that attach to the PELC, the median inception-point distance from the PELC tip and PELC attachment point increase with increasing return stroke peak current. Median leader-step progression speed is significantly (4.25 and 3.5 times, respectively) faster for the -104 and -228-kA return strokes than that of the -17-kA return stroke. Two factors that likely contribute to these discrepancies are the differences in leader characteristics for strokes with such remarkably different peak currents and the altitude AGL in which the leader-steps occur. Using modeling of leader-step formation, Cooray and Arevalo [18] predicted that the length of the streamer region ahead of the PELC tip, step length, and leader speed in negative cloud-to-ground lightning increase with increasing return stroke peak current. Kodali et al. [19] show the estimated line charge density for negative dart leaders to be positively correlated with return stroke peak currents in rocket-triggered lightning. If we assume this to be also the case for stepped leaders then strokes with higher peak currents are associated with leaders with higher line-charge-densities. It is likely that such leaders would produce streamer zones that extend farther ahead of the PELC-tip. If space leaders are assumed to form just at the edge of the PELC streamer zone (see e.g., Figure 1 of [20]), such high-line-charge-density leaders would result in space leaders forming at farther distances from the PELC-tip. Also, as the leader progresses from the reduced electric field region immediately below the

lower positive cloud charge region in a tripolar thundercloud to the enhanced field region closer to ground (see Figure 3 of [20]), its step-formation characteristics may change. As shown in Table II, our first and third stepped leaders (070420_17kA and 09062020_228kA, respectively) were recorded at similar altitude ranges (800 m – 1 km) AGL, while the second stepped leader (071020_104kA) was recorded at an altitude range (300-440 m) much closer to ground. According to the model predictions of Cooray and Arevalo [18], step lengths are expected to increase as the stepped leader approaches ground. This is likely the reason why the differences in space leader inception-point distances and lengths, as well as step-lengths, are much more pronounced between the first and second, and first and third stepped leaders in our dataset than those between the second and third stepped leaders. Also, the higher median leader speed for the second stepped leader than that of the third can probably be attributed to the lower altitude range at which it was observed.

ACKNOWLEDGMENT

The authors would like to acknowledge funding from the U.S. National Science Foundation Award 1934066 and U.S. Air Force contract FA252117P0079.

REFERENCES

[1] Gorin, B. N., Levitov, V. I., & Shkilev, A. V. (1976). Some Principles of Leader Discharge of Air Gaps with a Strong Non-uniform Field. Gas Discharges 143. IEE Conf. Publ., pp. 274–278.

[2] Biagi, C. J., Jordan, D. M., Uman, M. A., Hill, J. D., Beasley, W. H., & Howard, J. (2009). High speed video observations of rocket-and-wire initiated lightning. Geophysical Research Letters, 36, L15801. http://dx.doi.org/10.1029/2009GL038525

[3] Biagi, C. J., Uman, M. A., Hill, J. D., Jordan, D. M., Rakov, V. A., & Dwyer, J. (2010). Observations of stepping mechanisms in a rocket-and-wire triggered lightning flash. Journal of Geophysical Research: Atmospheres, 115, D23215. http://dx.doi.org/10.1029/2010JD014616

[4] Biagi, C. J., Uman, M. A., Hill, J. D., & Jordan, D. M. (2014). Negative leader step mechanisms observed in altitude triggered lightning. Journal of Geophysical Research: Atmospheres, 119, 8160–8168. http://dx.doi.org/10.1002/2013JD020281

[5] Hill, J. D., Uman, M. A., & Jordan, D. M. (2011). High-speed video observations of a lightning stepped leader. Journal of Geophysical Research: Atmospheres, 116, D16117. http://dx.doi.org/10.1029/2011JD015818

[6] Petersen, D. A., & Beasley, W. H. (2013). High-speed video observations of a natural negative stepped leader and subsequent dart-stepped-leader. Journal of Geophysical Research: Atmospheres, 118, 12,110–12,119. http://dx.doi.org/10.1002/2013JD019910

[7] Qi, Q., Lu, W., Ma, Y., Chen, L., Zhang, Y., & Rakov, V. A. (2016). High-speed video observations of the fine structure of a natural negative stepped leader at close distance. Atmospheric Research, 178-179, 260–267. https://doi.org/10.1016/j.atmosres.2016.03.027

[8] Jiang, R., Qie, X., Zhang, H., Liu, M., Sun, Z., Lu, G., Wang, Z., & Wang, Y. (2017). Channel branching and zigzagging in negative cloud-to-ground lightning. Scientific Reports, 7(1), 3457. https://doi.org/10.1038/s41598-017-03686-w

[9] Srivastava, A., Jiang, R., Yuan, S., Qie, X., Wang, D., Zhang, H., Sun, Z., & Liu, M. (2019). Intermittent propagation of upward positive leader connecting a downward negative leader in a negative cloud-to-ground lightning. Journal of Geophysical Research: Atmospheres, 124, 13763–13776. https://doi.org/10.1029/2019JD031148

[10] Qi, Q., Lyu, W., Ma, Y., Wu, B., Chen, L., Jiang, R., Zhu, Y., & Rakov, V. A. (2019). High-Speed video observations of natural lightning attachment process with framing rates up to half a million frames per second. Geophysical Research Letters, 46, 12,580–12,587. https://doi.org/10.1029/2019GL085072

[11] Nag, A., Murphy, M. J., Schulz, W., & Cummins, K. L. (2015). Lightning locating systems: Insights on characteristics and validation techniques. Earth and Space Science, 2, 65– 93. https://doi.org/10.1002/2014EA000051

[12] Nag, A., Mallick, S., Rakov, V. A., Howard, J. S., Biagi, C. J., Hill, J. D., Uman, M. A., Jordan, D. M., Rambo, K. J., Jerauld, J. E., DeCarlo, B. A., Cummins, K. L., & Cramer, J. A. (2011). Evaluation of U.S. National Lightning Detection Network performance characteristics using rocket-triggered lightning data acquired in 2004–2009. Journal of Geophysical Research: Atmospheres, 116, D02123. https://doi.org/10.1029/2010JD014929

[13] Mallick, S., Rakov, V. A., Hill, J. D., Ngin, T., Gamerota, W. R., Pilkey, J. T., Biagi, C. J., Jordan, D. M., Uman, M. A., Cramer, J. A., & Nag, A. (2014). Performance characteristics of the NLDN for return strokes and pulses superimposed on steady currents, based on rocket-triggered lightning data acquired in Florida in 2004–2012. Journal of Geophysical Research: Atmospheres, 119, 3825– 3856, https://doi:10.1002/2013JD021401

[14] Idone, V. P., Orville, R. E., Hubert, P., Barret, L., & Eybert-Berard, A. (1984). Correlated observations of three triggered lightning flashes. Journal of Geophysical Research: Atmospheres, 89, 1385–1394, https://doi.org/10.1029/JD089iD01p01385

[15] Gao, Y., Lu, W., Ma, Y., Chen, L., Zhang, Y., Yan, X., & Zhang, Y. (2014). Three-dimensional propagation characteristics of the upward connecting leaders in six negative tall-object flashes in Guangzhou. Atmospheric Research, Volume 149, 2014, Pages 193-203. https://doi.org/10.1016/j.atmosres.2014.06.008

[16] Wang, D., Takagi, N., Watanabe, T., Rakov, V. A., & Uman, M. A. (1999). Observed leader and return stroke propagation characteristics in the bottom 400 m of the rocket triggered lightning channel. Journal of Geophysical Research: Atmospheres, 104, 14,369–14,376. https://doi.org/10.1029/1999JD900201

[17] Gamerota, W. R., Idone, V. P., Uman, M. A., Ngin, T., Pilkey, J. T., & Jordan, D. M. (2014). Dart-stepped-leader step formation in triggered lightning. Geophysical Research Letters, 41, 2204–2211. https://doi.org/10.1002/2014GL059627

[18] Cooray, V., & Arevalo, L. (2017). Modeling the Stepping Process of Negative Lightning Stepped Leaders. Atmosphere 8, no. 12: 245. https://doi.org/10.3390/atmos8120245

[19] Kodali, V., Rakov, V. A., Uman, M. A., Rambo, K. J., Schnetzer, G. H., Schoene, J., & Jerauld, J. (2005). Triggered-lightning properties inferred from measured currents and very close electric fields. Atmospheric Research, 76, 355–376. https://doi.org/10.1016/j.atmosres.2004.11.036

[20] Nag, A., & Rakov, V. A. (2016). A unified engineering model of the first stroke in downward negative lightning. Journal of Geophysical Research: Atmospheres, 121, 2188–2204. https://doi.org/10.1002/2015JD023777